

# Plasmon nano-optical tweezers

Mathieu L. Juan<sup>1</sup>, Maurizio Righini<sup>1</sup> and Romain Quidant<sup>1,2</sup>

**Conventional optical tweezers, formed at the diffraction-limited focus of a laser beam, have become a powerful and flexible tool for manipulating micrometre-sized objects. Extending optical trapping down to the nanometre scale would open unprecedented opportunities in many fields of science, where such nano-optical tweezers would allow the ultra-accurate positioning of single nano-objects. Among the possible strategies, the ability of metallic nanostructures to control light at the subwavelength scale can be exploited to engineer such nano-optical traps. This Review summarizes the recent advances in the emerging field of plasmon-based optical trapping and discusses the details of plasmon tweezers along with their potential applications to bioscience and quantum optics.**

To understand the limitations faced by conventional optical tweezers<sup>1–4</sup> when dealing with nanometre-sized specimens, we first consider an object of radius  $R$  much smaller than the wavelength of the incident trapping light (known as the Rayleigh regime). Reducing the size of the object causes two main effects that both work against stable trapping. First, the magnitude of the restoring force decreases abruptly (following an  $R^3$  law), which results in a shallower trapping well. Second, the damping of the trapped specimen decreases because of a reduction in viscous drag. Both effects alter the confinement of the specimen within the trap, as illustrated in Fig. 1a–d. For a fixed average thermal energy  $k_B T$  (where  $k_B$  is the Boltzmann constant and  $T$  is the absolute temperature in the trap), this increasing delocalization allows the specimen to escape from the trap.

To compensate for this delocalization and prevent the specimen from escaping, one can either increase the trap confinement by further focusing the trapping laser light or augment the depth of the trapping potential by increasing the local laser intensity experienced by the specimen. The rule of thumb, established by Ashkin in his seminal work<sup>1</sup>, states that stable trapping requires a potential depth of around  $10k_B T$  to compensate for stochastic kicks in the particle's Brownian motion.

Although diffraction prevents the confinement of propagating light beyond a fraction of its wavelength, recent advances in nanooptics have led to alternative techniques based on nano-optical tweezers that are capable of trapping and manipulating nanometre-sized objects. Indeed, unlike propagating fields, evanescent fields can be concentrated well beyond the diffraction limit<sup>5,6</sup>. Among the different approaches, plasmon nano-optics<sup>7–9</sup>, which exploits the surface plasmon resonances supported by metallic nanostructures (Box 1), is particularly efficient in controlling light down to the nanometre scale<sup>10–12</sup>. Plasmonic nanostructures can be engineered to efficiently couple to propagating light and concentrate it into highly localized and intense optical fields known as hot spots (Fig. 1e)<sup>13–16</sup>. By simultaneously increasing the confinement and augmenting the depth of the trapping potential, plasmonics opens up many new opportunities for optical trapping at the nanometre-scale.

This Review summarizes recent research that lies at the crossing point between plasmon optics and optical manipulation. First we examine the various implementations of plasmon-based trapping and how they are different to conventional optical tweezers. We then discuss how surface plasmon traps may lead to novel nanotools that could allow exciting new experiments in various fields of science.

## Surface plasmons and optical forces

In the early years of research into near-field optics, several theoretical proposals were made regarding the use of evanescent fields for optical trapping<sup>17–28</sup>. Novotny *et al.*<sup>21</sup> and Martin *et al.*<sup>22</sup> suggested exploiting the subwavelength light concentration at the extremity of a sharp metallic tip to create a nano-optical trap able to immobilize dielectric objects as small as a few tens of nanometres. At around the same time, Kawata *et al.* proposed a similar approach that produced a nano-optical trap using the confined light transmitted through a nanoaperture in an opaque metallic film<sup>23</sup>. In both configurations, the interaction of the propagating incident laser with the nanostructure was predicted to create large  $k$ -vectors characteristic of evanescent waves, resulting in the subwavelength concentration of light (Fig. 1e). In other words, the illuminated nanostructure functions as a nanolens that is capable of concentrating light well beyond that of a high-numerical-aperture objective lens in a microscope. Interestingly, such nanostructure-assisted formation of the optical potential makes it possible to create a complex near-field landscape from a single beam, including a large number of nanometre-sized traps for the parallel trapping of multiple nano-objects at predefined locations on a surface<sup>28</sup>. Another attractive advantage of using a structured surface is its potential integrability into a compact platform without any need for bulky optical elements. However, the use of a fixed plasmonic pattern *a priori* limits the possibility of manipulating the object in three dimensions.

Experimental research on surface plasmon (SP)-based trapping was triggered by two pioneering studies into the enhanced force field at a homogeneous gold/water interface supporting a surface plasmon polariton (SPP). In 2006, Garcés-Chávez and co-workers reported the self-assembly of a large number of micrometre-sized dielectric beads within the region of a gold surface where an SPP was excited<sup>29</sup>. The same year, Volpe *et al.* used photonic force microscopy to probe the SPP force field, and measured a 40-fold enhancement to the force magnitude<sup>30</sup>.

## Plasmonic microtrapping

Although a homogeneous metallic film illuminated by an unfocused laser beam has a homogeneous optical force field, stable trapping at a predefined location on the film surface requires a confined trapping well, which can be achieved through metal patterning. The first experimental implementation of SP-based trapping was demonstrated using a glass surface decorated by micrometre-sized gold disks<sup>31,32</sup>. In this experiment, the patterned surface was illuminated through a glass prism (known as the Kretschmann

<sup>1</sup>ICFO-Institut de Ciències Fotoniques, Mediterranean Technology Park, 08860 Castelldefels (Barcelona), Spain. <sup>2</sup>ICREA-Institució Catalana de Recerca i Estudis Avançats, 08010 Barcelona, Spain. e-mail: romain.quidant@icfo.es

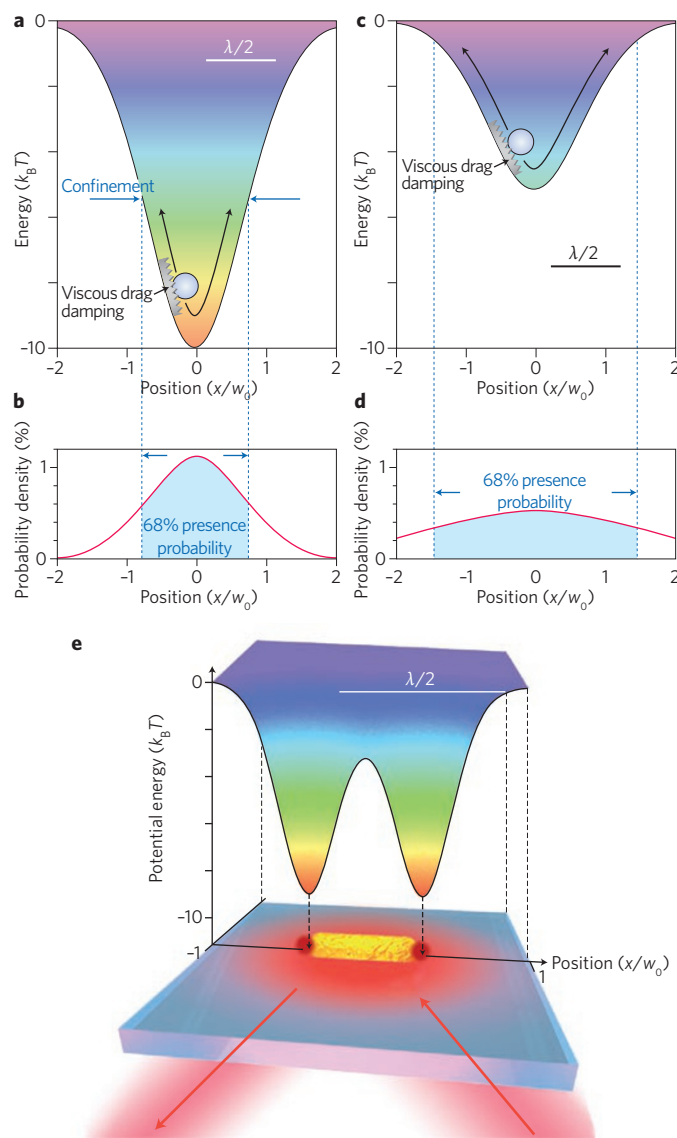


**Figure 1 | Conventional optical trapping versus surface plasmon trapping.**

**a,b**, Trapping potential (**a**) and associated position distribution (**b**) for a polystyrene sphere of radius  $R$ . **c,d**, Trapping potential (**c**) and associated position distribution (**d**) for a polystyrene sphere of radius  $0.8R$ . The ratio between **a** and **b** is identical to that between **c** and **d**. Comparing **a** and **b** with **c** and **d** shows the dramatic impact that results from a size reduction of only 20%. **e**, Optical potential landscape resulting from the illumination of a gold nanostructure. The half-wavelength bar in panels **a**, **c** and **e** gives an approximate scale of reference.

configuration) by an unfocused ( $\sim 100 \mu\text{m}$  waist), linearly *p*-polarized near-infrared laser beam (Fig. 2a). The gold pattern was covered by a static fluidic chamber containing a diluted aqueous suspension of micrometre-sized polystyrene beads. When the direction of the incident light matched the SPP resonance angle, the light efficiently coupled to the SPP mode supported by the top gold/water interface. Owing to the combined effects of the boundaries and asymmetrical illumination, the plasmonic field was concentrated in the forward portion of the disk. No solution flow was used; it was the incident evanescent field that pushed the polystyrene beads at the glass–water interface along the incident in-plane  $k$ -vector, thus guiding them towards the trapping region of the surface. Figure 2b shows how a bead passing over one of the

### Box 1 | SPPs versus LSPs.

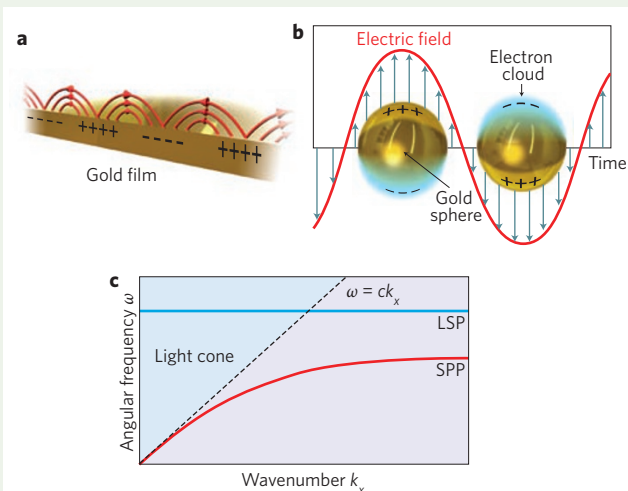


**Figure B1 | Illustration of SPPs and LSPs, together with their associated dispersion diagrams.** **a,b**, Collective oscillation of electrons with the incident electromagnetic field at a flat gold–air interface (SPP); **a**) and in a gold nanoparticle (LSP; **b**). **c**, Typical dispersion curves of SPPs (red) and LSPs (blue).

Two distinct types of surface plasmons are known to exist, depending on the geometry of the metal. SPPs sustained at a flat metal–dielectric interface are propagating electromagnetic surface waves associated with a collective oscillation of the free electrons in the metal driven by the electromagnetic field. Because SPPs are pure evanescent modes decaying exponentially away from the interface, they cannot be directly coupled to propagating light and thus a technique is required to compensate for the momentum mismatch. This is usually done by illuminating a thin metal film under total internal reflection through a glass prism of higher refractive index than the dielectric. Efficient coupling to an SPP mode enables light at the metal surface to be concentrated into an intense and confined surface wave whose intensity is dramatically larger than the incident intensity.

Unlike SPPs on flat and extended metal interfaces, LSPs are associated with bound electron plasmas in nanovoids or particles with dimensions much smaller than the incident wavelength. SPPs have a continuous dispersion relation and therefore exist over a wide range of frequencies, but LSP resonances exist only over a finite frequency range owing to the additional constraints imposed by their finite dimensions. The spectral position of this resonance is governed by the particle's size and shape, as well as by the dielectric functions of both the metal and the surrounding media. LSPs can be directly coupled with propagating light, whereas SPPs cannot.

pads gets trapped in a forwards position, where the SPP field intensity is expected to be maximum. Trapping times of up to several hours were achieved for an incident laser intensity of  $10^7 \text{ W m}^{-2}$  — around two orders of magnitude smaller than that required to trap a bead of the same size through conventional optical tweezers. To demonstrate that trapping is triggered by the pad plasmon resonance and rule out any sticking effects, the linear polarization of the illumination can be switched from *p* to *s*, for which light does not couple to the SPP. The resulting strong decrease in the near-

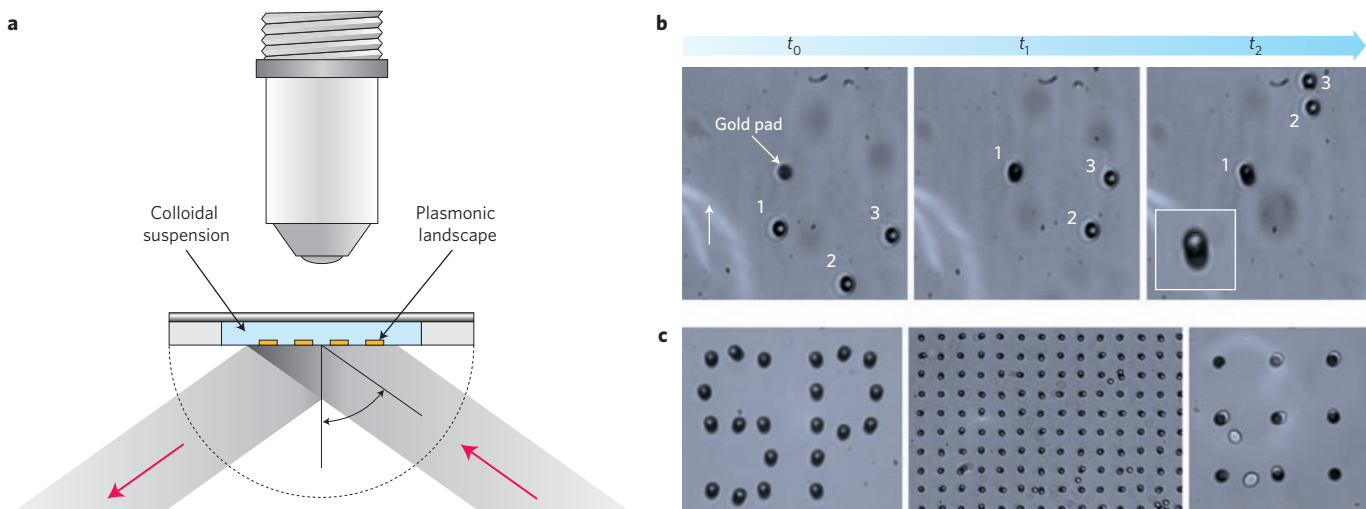


**Figure 2 | SP-based microtrapping.** **a**, Schematic of the experimental set-up, in which a pattern of micrometre-sized gold disks is illuminated under the Kretschmann configuration through a glass prism. The black arrow gives the direction of the incident in-plane  $k$ -vector. **b**, Frame sequence illustrating the trapping of a 4.8  $\mu\text{m}$  polystyrene bead in the forward position of a gold disk<sup>32</sup>. **c**, Parallel trapping of polystyrene beads and yeast cells using a single laser beam<sup>31</sup>.

field intensity at the gold surface makes the optical well shallower, hence releasing the bead. As mentioned above, because the pad is much smaller than the illumination spot, the experiment can be extended to an ensemble of pads to achieve, under the same illumination conditions, parallel trapping of a large number of beads (Fig. 2c). Beyond this proof-of-concept, parallel SP trapping provides potential new techniques for the manipulation of living cells (Fig. 2c, right) by investigating their response to external stimuli. In this research direction, Martin *et al.* recently reported the parallel trapping of yeast cells in a microfluidic circuit<sup>33</sup>.

In addition to being well-suited for integration on a chip, the in-plane geometry of SP traps provides them with some particularly attractive features. Similar to conventional three-dimensional optical tweezers, the trapping mechanism in SP tweezers relies on a suitable balance between scattering and gradient forces. Owing to the 2D geometry of SP traps, both the scattering (repulsive) and the gradient (attractive) forces are contained within the surface plane. However, in contrast with three-dimensional optical tweezers, both force contributions in SP trapping depend on illumination parameters such as the direction and polarization of the incident light. On the one hand, the magnitude of the scattering force increases as the angle decreases<sup>17</sup>, but on the other hand, the incident angle also controls the gradient force component when scanning across the pad SPP resonance. Consequently, the trapping properties of SP traps can be tuned by changing the balance between the two competing force components. Such tuning has been exploited to selectively trap one particle size out of a mix of several sizes<sup>32</sup>.

Although a purely electromagnetic model is sufficient to explain the trapping mechanism of SP tweezers, it is important to mention that optical forces may also coexist with thermally induced forces. In addition to optical gradients, coupling to SP resonances leads to local heating of the metal and heat dissipation to the surrounding fluid, which results in convection and thermophoresis<sup>29</sup>. It was experimentally observed that the contribution of convection could be minimized by reducing the metal density (by exploiting well-separated gold disks) and using thin fluidic chambers with thicknesses smaller than 20  $\mu\text{m}$  (ref. 29). So far there has been no clear data to quantify the respective contributions of optical and thermal effects.

### Subwavelength trapping with plasmonic antennas

Although the simple disk geometry enables dielectric beads as small as 1  $\mu\text{m}$  to be trapped by down-scaling the pad diameter accordingly, it fails for smaller sizes. At the heart of this failure is the change in nature of SPs when the disk becomes commensurable with or smaller than the SP wavelength. Owing to boundary effects, subwavelength gold structures support localized surface plasmon (LSP) resonances, which differ in several ways from SPPs in an extended film (see Box 1). Although gold pads measuring around 100 nm can be designed to be resonant in the near-infrared region of the spectrum, they are not suited for trapping because of their limited intensity and symmetry in the optical near field<sup>28</sup>.

Much higher control of plasmonic fields can be achieved through an alternative technique that exploits the strong electromagnetic coupling between several adjacent plasmonic nanostructures. Among the most interesting geometries, plasmonic antennas (also known as plasmonic dimers) have received much attention for their ability to concentrate propagating light well beyond the diffraction limit<sup>34–36</sup>. Gap antennas usually consist of two identical metallic particles separated by a nanoscale dielectric gap. When the incident field is linearly polarized along the vector connecting the particles, capacitive effects lead to a confined and intense light spot within the gap region. Their huge potential for enhancing light–matter interactions at the nanoscale have raised the expectations of gap antennas in fields such as data processing<sup>37</sup>, spectroscopy and sensing<sup>38–40</sup>, and nonlinear optics<sup>41</sup>.

The ability of gap antennas to concentrate laser light into very localized and intense hot spots makes them particularly attractive for creating optical traps orders of magnitude smaller than those achievable through the original pad approach, enabling SP trapping to be extended to the nanometre scale. Numerical calculations by Xu *et al.* first predicted that hot spots in the gaps of metallic dimers could increase the residence time of single molecules in surface-enhanced Raman spectroscopy experiments<sup>42</sup>.

As a first experimental step in this direction, Grigorenko *et al.* recently used gap antennas to assist conventional optical tweezers<sup>43</sup>. In their experiment, a 200 nm polystyrene bead, trapped in a viscous medium at the tight focus of a 1,064 nm laser beam, was brought in close proximity to a surface patterned with pairs of gold cylinders designed to be resonant at the same wavelength.

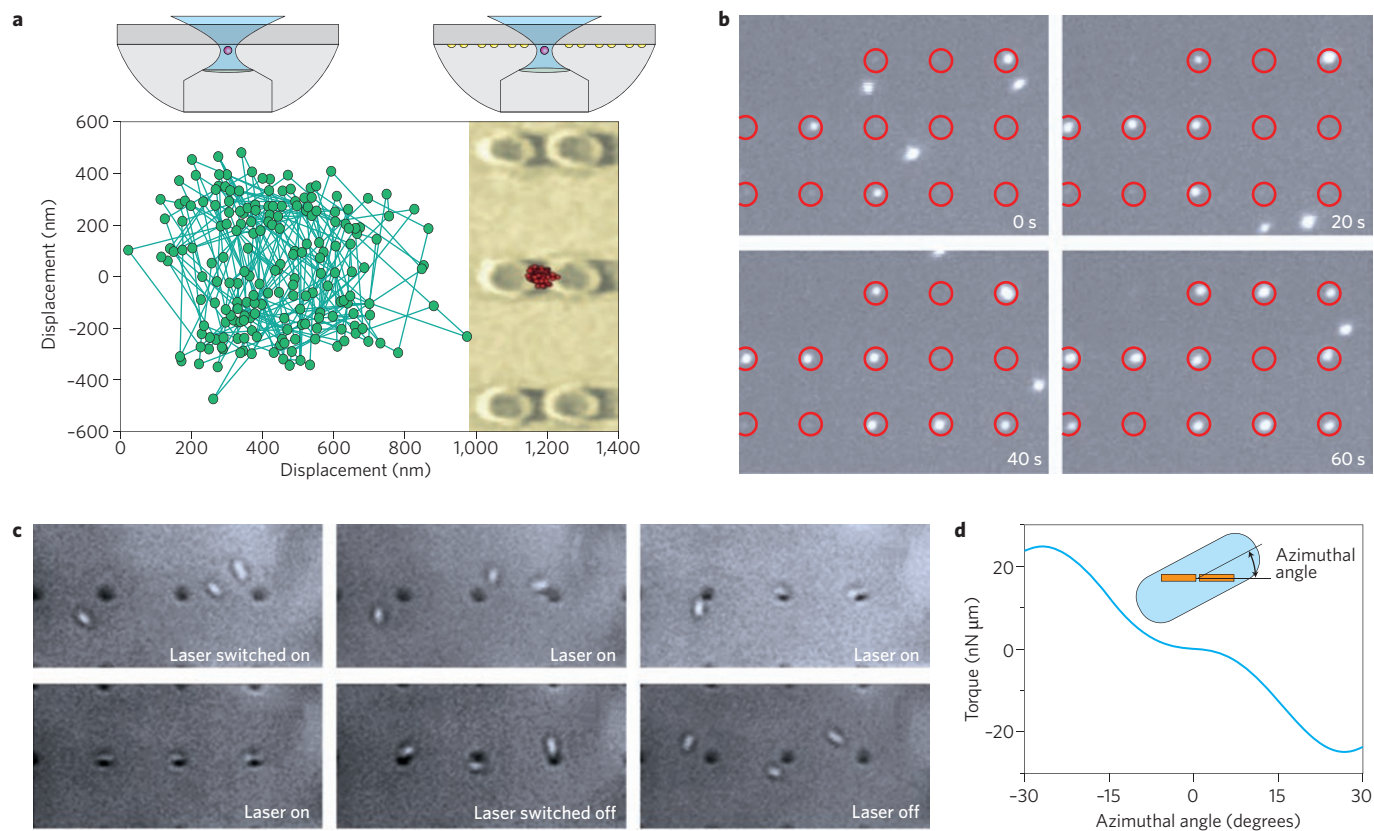


**Figure 3 | Antenna trapping.** **a**, Gap antennas formed by two adjacent gold nanoparticles can assist conventional optical tweezers to reduce the spatial confinement of 200 nm polystyrene beads down to subwavelength dimensions<sup>43</sup>. **b**, Parallel SP trapping of 200 nm polystyrene beads in an array of gap nano-antennas illuminated by an unfocused beam<sup>44</sup>. **c,d**, Parallel trapping and alignment of *Escherichia coli* bacteria (**c**) and calculated torque experience by the bacteria when exposed to the antenna force field (**d**)<sup>44</sup>. Figure reproduced with permission from: **a**, ref. 43, © 2008 NPG; **b-d**, ref. 44, © 2009 ACS.

As illustrated in Fig. 3a, exposing the bead to the antenna hot spot modifies the overall optical potential seen by the bead, leading to a reduction in the trapping volume beyond the diffraction limit and thus providing an order-of-magnitude increase in bead confinement. In addition, the trapped object can be transferred between adjacent antennas by translating the laser beam, which allows the object to be discretely positioned.

Shortly after the work of Grigorenko *et al.*, antennas were used as autonomous on-chip nano-optical traps capable of operating without the use of auxiliary conventional optical tweezers<sup>44</sup>. Righini *et al.* achieved parallel trapping of 200 nm polystyrene beads in aqueous solution using unfocused illumination and an array of gap antennas formed by adjacent gold nanobars<sup>44</sup> (Fig. 3b). Such geometry supports a high-order resonance in the near-infrared that leads to a main hot spot within the gap and secondary hot spots along the bars and at their outer extremities. The applicability of this configuration to biological samples has also been demonstrated on living *Escherichia coli* bacteria. Interestingly, in addition to being efficiently trapped, the bacteria systematically align along the long axis of the antenna (Fig. 3c,d). This effect is due to the elongated shape of the bacteria, which enables them to exploit several trapping sites along the antenna until stabilized in a minimum-energy equilibrium position. Using a complex optical potential landscape formed by multiple nano-trapping sites to achieve further immobilization and controlled orientation is the nanoscale equivalent of multiple-beam trapping implemented with conventional optical tweezers for the accurate manipulation of cells<sup>45,46</sup>. Stabilizing the specimen in the trap allows it to be optically inspected using techniques that require significant acquisition times, such as Raman spectroscopy<sup>47,48</sup>.

### Self-induced back-action trapping

Although enhanced and confined plasmonic fields allow dramatically strong field gradients and large local intensities to be achieved, previously discussed schemes suffer from a practical limitation that prevents trapping beyond a certain size. Indeed, one unavoidably reaches a limit above which the required intensity causes heat damage to the trapped specimen and/or the metallic structure<sup>1</sup>. Even when not reaching such extreme limits, the thermal effects associated with intense fields may play an increasing role in the object's dynamics, and in some cases dominate over optical forces.

Extending optical trapping towards the nanometre regime therefore requires additional refinements to the trapping mechanism. The usual approach for optical trapping relies on a static picture, in which the potential well is optimized for a given object and remains constant over the experiment; that is, no modifications are applied to the potential well to account for the stochastic aspect of Brownian motion. Although the average kinetic energy of the object within the trap is given by  $k_B T$ , the instantaneous velocity follows a Maxwell–Boltzmann distribution<sup>49</sup>, in which the object energy can occasionally significantly exceed the average value. Potential depths of around  $10k_B T$  are typically used to compensate for these high-energy events<sup>1</sup>; a depth of  $k_B T$  would only hold the object until a high-energy event occurs.

Conversely, a dynamical approach, in which the trapping potential is dynamically reconfigured to compensate for high-energy events, would enable the required average trap depth to be strongly reduced. With this aim, external real-time feedback techniques have been applied to conventional optical tweezers to correct the trapping potential by adjusting either the laser intensity<sup>50</sup> or the trap

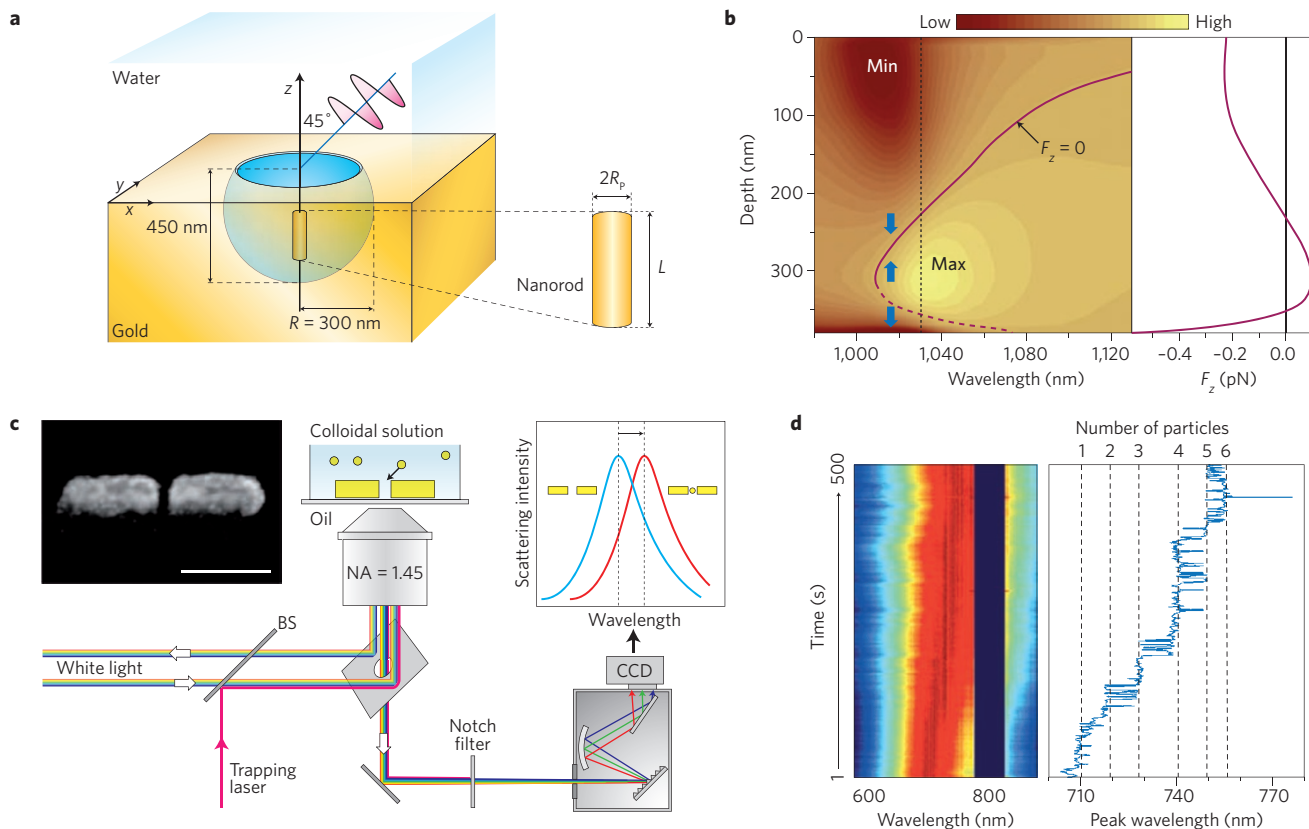


**Figure 4 | Plasmonic nanotrapping based on a trap–specimen interaction.** **a**, Trapping of a gold nanorod of radius  $R_p$  in a metallic nanovoid. **b**, The computed dependence with the incident wavelength of the vertical force component ( $F_z$ ) experienced by the nanorod shows changes in its equilibrium position<sup>59</sup>. **c**, Trapping of gold nanoparticles in the gap of a gold antenna. NA, numerical aperture; BS, beamsplitter; CCD, charge-coupled device. **d**, Monitoring the antenna resonance shift allows trapping events to be monitored and the number of trapped nanoparticles to be discriminated<sup>60</sup>. The peak wavelength shift allows the number of trapped particles (one, two, three, four, five or six objects in **d**) to be discriminated. Figure reproduced with permission from: **a,b**, ref. 59, © 2008 APS; **c,d**, ref. 60, © 2010 ACS.

position<sup>51</sup>. In practice, external feedback increases the effective stiffness of the trap<sup>52</sup>, producing a force clamp<sup>51</sup> and allowing the object to be further confined by adding an external source of damping<sup>50</sup>. Although this approach relaxes the requirements on the local intensity within the trap, thereby reducing the likelihood of optical damage<sup>52</sup>, it relies on a complex auxiliary feedback set-up with a limited bandwidth, and is therefore sensitive to position measurement errors.

Alternatively, the extreme sensitivity of plasmonic nanostructures to their environment can be exploited to achieve some control over the features of an SP trap. The dependence of plasmon resonances to tiny changes of refractive index in the surrounding material has been extensively exploited to design efficient and compact sensors for gas, liquid and biomolecule detection<sup>53–57</sup>. In the context of optical trapping, this sensitivity can have a destructive impact whenever the presence of the trapped object in the trapping site reduces the field gradient and/or the local intensity, as observed in ref. 58.

Conversely, plasmonic structures can also be devised such that the trapped object induces a constructive effect that favours trapping. García de Abajo and co-workers theoretically proposed exploiting the sensing ability of plasmonic nanostructures to achieve a reconfigurable nanotrap<sup>59</sup> (Fig. 4a,b). In this configuration, a gold nanorod is trapped in the strong local field of a microvoid drilled in a gold film. Because the distribution and spectrum of the microvoid mode depend strongly on the nanorod position, the trapping equilibrium position can be tuned by changing the illumination wavelength. More recently, Zhang and co-workers reported efficient trapping of

single gold nanoparticles within the gap of a gold antenna. Owing to their conductivity and high polarizability (about one order of magnitude higher than a polystyrene bead of the same size), gold nanoparticles have a strong impact on the gap antenna resonance by somehow shortcircuiting its two arms<sup>60</sup>. Interestingly, the induced resonance shift allows the presence of the particle within the trap to be monitored (Fig. 4c,d).

Further steps involve fully exploiting the trap–specimen interaction to achieve an automatic feedback control that does not require any external monitoring or correcting. For this, one first aims to optimize the trapping efficiency by properly engineering the plasmonic mode such that the local intensity within the trap is maximized when the object is present. As a consequence, the momentum of the (plasmonic) photons interacting with the object experiences significant changes as the object moves in and out of the trap. Owing to momentum conservation, these changes create an additional dynamical force field that is by definition automatically synchronized with the object’s dynamics. This ‘self-induced back-action’ (SIBA) was recently demonstrated using a nanoaperture in a metallic film<sup>61</sup>.

SIBA trapping based on metallic nanoapertures<sup>62–64</sup> relies on the high sensitivity of the aperture transmission to its dielectric environment. The presence of an object within the aperture, where the mode is confined, modifies the effective refractive index, hence red-shifting the transmission spectrum<sup>65</sup>. Using a red-detuned laser such that the local field enhancement in the aperture gets stronger when the object is trapped leads to automatic positive back-action.

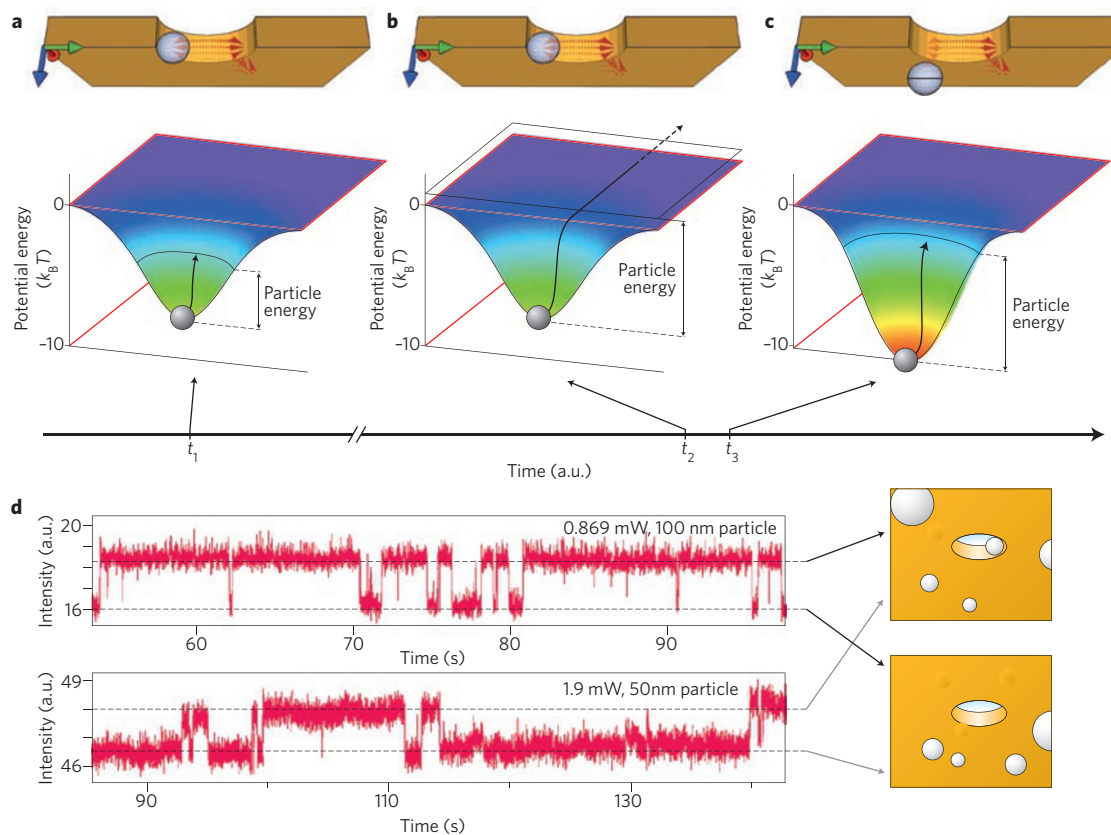


**Figure 5 | SIBA trapping.** **a**, The particle is localized in the aperture at time  $t_1$  while having moderate kinetic energy. **b**, During a high-energy event at time  $t_2$ , the object can escape the aperture. **c**, As the particle moves out of the aperture at time  $t_3$ , the SIBA force increases the potential depth to maintain the object within the trap. **d**, Experimental transmission intensity time trace showing trapping of 100 nm and 50 nm polystyrene beads in a 310 nm aperture drilled in a gold film<sup>61</sup>. Figure **d** reproduced with permission from ref. 61, © 2011 NPG.

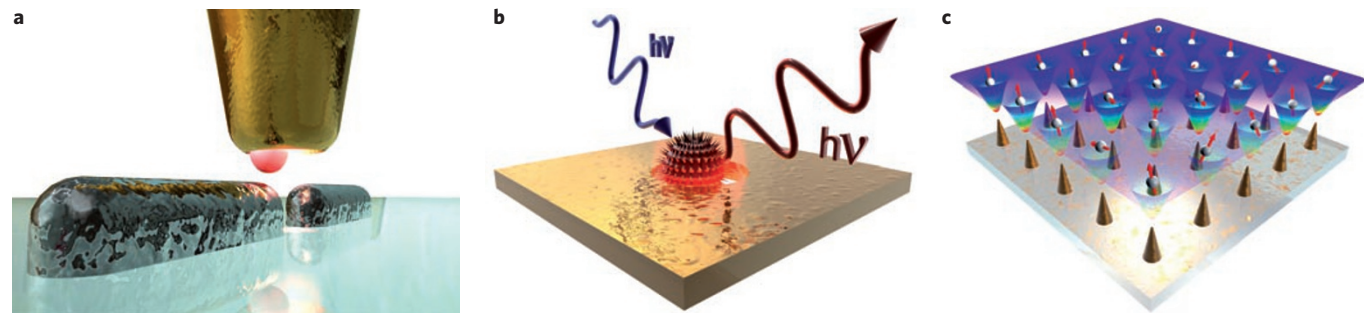


**Figure 6 | Future outlook and applications.** **a**, The extension of SIBA trapping at the extremity of an elongated optical fibre would allow nano-objects such as single emitters to be positioned with nano-accuracy near optical systems of interest. **b**, Owing to its low intensity requirements, SIBA optical trapping should allow the trapping of nanoscale living biological specimens such as viruses to perform on-chip optical diagnostics. **c**, Large-scale parallel SP trapping would also enable a large number of single atoms to be arranged, thus providing a new scalable platform for exploring many-body physics.

Whenever the total photon momentum travelling through the aperture decreases as the object escapes the trap, the SIBA force, pointing towards the equilibrium position, slows it down. This allows the incident laser intensity to be reduced to values associated with a potential depth of the order of  $k_B T$ . The SIBA restoring force automatically increases the effective trapping potential depth during high-energy events to maintain the object within the trap, as illustrated in Fig. 5a–c. The SIBA effect has recently allowed efficient trapping of 100 nm and 50 nm polystyrene spheres with incident laser powers as low as 1 mW at a focus spot size of  $1 \mu\text{m}^2$  (Fig. 5d)<sup>61</sup>. This approach shows a striking departure from previous techniques<sup>66–68</sup>. Although originally demonstrated with nanoapertures in a metallic film, the

SIBA approach relies on a more general phenomenon and could be applied to a large variety of geometries. In particular, recent efforts in the field of sensing based on the latest advances in plasmon nanooptics and metamaterials<sup>69–73</sup> could significantly benefit from the optimization of SIBA traps. Careful optimization of the spatial overlap between the plasmonic mode and the trapped object, combined with an increase in the mode quality factor, should soon enable non-invasive single virus or protein trapping.

### Future outlook and applications

**SP nano-tweezers in future integrated analytical devices.** Beyond their interest for performing unprecedented basic experiments,

SP nanotweezers may play a key role in the development of future integrated analytical platforms, known as 'lab-on-a-chip' (Fig. 6b). Although current technology in the field of microfluidics enables routing cells for single-cell flow cytometry, SP trapping could become an important tool for immobilizing flowing cells for a period of time that allows them to be inspected optically. The combination of specimen-selective SP trapping and SP-enhanced spectroscopy could lead, for instance, to the efficient screening of tumour cells.

**From nanotraps to nanotweezers.** SP traps formed by nanostructured surfaces have proven to be a powerful strategy for immobilizing single or multiple nano-objects on a substrate. However, ultra-accurate three-dimensional manipulation of the trapped specimen is also a highly desirable technique, for instance to position a single nano-emitter near a micro- or nano-optical structure of interest. Although the original idea of using a bulk metallic tip<sup>21</sup> has not yet been demonstrated experimentally, SIBA trapping could be implemented at the extremity of an elongated coated optical fibre to minimize thermally induced effects (Fig. 6a).

**Quantum information.** Far from applications in biosciences, the nano-accuracy of SP nanotweezers could strongly benefit research in quantum optics based on cold neutral atoms. Recent advances in laser-cooled atoms have raised expectations in the field of quantum information and atom optics. Despite the latest developments in integrated atom traps, which usually combine optical and magnetic force fields, further miniaturization and accuracy in the immobilization and manipulation of single, cold atoms remains highly desirable. Several theoretical works have studied the feasibility of creating a single-atom nanotrap at the extremity of a sharply elongated optical near-field tip. Unlike dielectric beads or biological specimens, atoms must remain far enough away from the metal in order to prevent their adsorption. This can be achieved, for example, by using blue-detuned trapping in a minimum of the field intensity<sup>74–76</sup>. Although similar results should be achievable near a surface patterned with plasmonic antennas or nanoapertures, the near-field probe approach combines the scanning ability with direct far-field interfacing to efficiently couple photons into and out of the trapped atom. This would allow the atom to be accurately positioned near a micro- or nano-photonic structure, or another atom. Furthermore, on-chip arrays of nanotraps with very short lattice constants, as illustrated in (Fig. 6c), could allow us to study their collective coherent interaction and explore novel many-body physics.

## References

1. Ashkin, A., Dziedzic, J. M., Bjorkholm, J. E. & Chu S. Observation of a single-beam gradient force optical trap for dielectric particles. *Opt. Lett.* **11**, 288–290 (1986).
2. Grier, D. A revolution in optical manipulation. *Nature* **424**, 810–816 (2003).
3. Neuman K. C. & Block S. M. Optical trapping. *Rev. Sci. Instrum.* **75**, 2787–2809 (2004).
4. Dholakia, K. & Reece, P. Optical micromanipulation takes hold. *Nano Today* **1**, 18–27 (2006).
5. Vigoureux, J. M. & Courjon, D. Detection of nonradiative fields in the light of the Heisenberg uncertainty principle and the Rayleigh criterion. *Appl. Opt.* **31**, 3170–3177 (1992).
6. Novotny, L. & Hecht, B. *Principles of Nano-Optics* Ch. 4 (Cambridge Univ., 2006).
7. Raether, H. *Excitation of Plasmons and Interband Transitions by Electrons* Ch. 1 (Springer, 1980).
8. Kreibig, U. & Vollmer, M. *Optical Properties of Metal Clusters* Ch. 2 (Springer, 1997).
9. Maier, S. *Plasmonics: Fundamentals and Applications* Ch. 5 (Springer, 2007).
10. Barnes, W. L., Dereux, A. & Ebbesen, T. W. Surface plasmon subwavelength optics. *Nature* **424**, 824–830 (2003).
11. Ozbay, E. Plasmonics: merging photonics and electronics at nanoscale dimensions. *Science* **311**, 189–193 (2006).
12. Schuller, J. A. *et al.* Plasmonics for extreme light concentration and manipulation. *Nature Mater.* **9**, 193–204 (2010).
13. Shalaev, V. M. & Sarychev, A. K. Nonlinear optics of random metal–dielectric films. *Phys. Rev. B* **57**, 13265–13288 (1998).
14. Gresillon, S. *et al.* Experimental observation of localized optical excitations in random metal–dielectric films. *Phys. Rev. Lett.* **82**, 4520–4523 (1999).
15. Li, K., Stockman, M. I. & Bergman, D. J. Self-similar chain of metal nanospheres as an efficient nanolens. *Phys. Rev. Lett.* **91**, 227402 (2003).
16. Stockman, M. I. Nanofocusing of optical energy in tapered plasmonic waveguides. *Phys. Rev. Lett.* **93**, 137404 (2004).
17. Kawata, S. & Sugiura, T. Movement of micrometer-sized particles in the evanescent field of a laser beam. *Opt. Lett.* **17**, 772–774 (1992).
18. Girard, C., Dereux, A. & Martin, O. J. F. Theoretical analysis of light-inductive forces in scanning probe microscopy. *Phys. Rev. B* **49**, 13872–13881 (1994).
19. Dereux, A., Girard, C., Martin O. J. F. & Devel, M. Optical binding in scanning probe microscopy. *Europhys. Lett.* **26**, 37–42 (1994).
20. Kawata, S. & Tani, T. Optically driven Mie particles in an evanescent field along a channelled waveguide. *Opt. Lett.* **21**, 1768–1770 (1996).
21. Novotny, L., Bian, R. X. & Xie, X. S. Theory of nanometric optical tweezers. *Phys. Rev. Lett.* **79**, 645–648 (1997).
22. Martin, O. J. F. & Girard, C. Controlling and tuning strong optical field gradients at a local probe microscope tip apex. *Appl. Phys. Lett.* **70**, 705–707 (1997).
23. Okamoto, K. & Kawata, S. Radiation force exerted on subwavelength particles near a nanoaperture. *Phys. Rev. Lett.* **83**, 4534–4537 (1999).
24. Chaumet, P., Rahmani, A. & Nieto-Vesperinas, M. Optical trapping and manipulation of nano-objects with an apertureless probe. *Phys. Rev. Lett.* **88**, 123601 (2002).
25. Nieto-Vesperinas, M., Chaumet, P. & Rahmani, A. Near field photonic forces. *Phil. Trans. R. Soc. A* **362**, 719–737 (2004).
26. Gu, M., Haumont, J. B., Micheau, Y., Chon, J. W. M. & Gan, X. Laser trapping and manipulation under focused evanescent wave illumination. *Appl. Phys. Lett.* **84**, 4236–4238 (2004).
27. Cizmar, T., Garcés-Chávez, V., Dholakia, K. & Zemánek, P. Optical conveyor belt for delivery of submicron objects. *Appl. Phys. Lett.* **86**, 174101 (2005).
28. Quidant, R., Petrov, D. & Badenes, G. Radiation forces on a Rayleigh dielectric sphere in a patterned optical near field. *Opt. Lett.* **30**, 1009–1011 (2005).
29. Garcés-Chávez, V. *et al.* Extended organization of colloidal microparticles by surface plasmon polariton excitation. *Phys. Rev. B* **73**, 085417 (2006).
30. Volpe, G., Quidant, R., Badenes, G. & Petrov, D. Surface plasmon radiation forces. *Phys. Rev. Lett.* **96**, 238101 (2006).
31. Righini, M., Zelenina, A. S., Girard, C. & Quidant, R. Parallel and selective trapping in a patterned plasmonic landscape. *Nature Phys.* **3**, 477–480 (2007).
32. Righini, M., Volpe, G., Girard, C., Petrov, D. & Quidant, R. Surface plasmon optical tweezers: tunable optical manipulation in the femtonewton range. *Phys. Rev. Lett.* **100**, 183604 (2008).
33. Huang, L., Maerk, S. J. & Martin, O. J. F. Integration of plasmonic trapping in a microfluidic environment. *Opt. Express* **17**, 6018–6024 (2009).
34. Mühlischlegel, P., Eisler, H. J., Martin, O. J. F., Hecht, B. & Pohl, D. W. Resonant optical antennas. *Science* **308**, 1607–1609 (2006).
35. Schuck, P. J., Fromm, D. P., Sundaramurthy, A., Kino, G. S. & Moerner, W. E. Improving the mismatch between light and nanoscale objects with gold bowtie nanoantennas. *Phys. Rev. Lett.* **94**, 017402 (2005).
36. Aizpurua, J. *et al.* Optical properties of coupled metallic nanorods for field-enhanced spectroscopy. *Phys. Rev. B* **71**, 235420 (2005).
37. Tang, L. *et al.* Nanometre-scale germanium photodetector enhanced by a near-infrared dipole antenna. *Nature Photon.* **2**, 226–229 (2008).
38. Kinkhabwala, A. *et al.* Large single-molecule fluorescence enhancements produced by a bowtie nanoantenna. *Nature Photon.* **3**, 654–657 (2009).
39. Acimovics, S., Kreuzer, M. P., Gonzalez, M. U. & Quidant, R. Plasmon near-field coupling in metal dimers as a step toward single-molecule sensing. *ACS Nano* **3**, 1231–1237 (2009).
40. Garcia-Parajo, M. F. Optical antennas focus in on biology. *Nature Photon.* **2**, 201–203 (2008).
41. Kim, S. *et al.* High-harmonic generation by resonant plasmon field enhancement. *Nature* **453**, 757–760 (2008).
42. Xu, H. & Käll, M. Surface-plasmon-enhanced optical forces in silver nanoaggregates. *Phys. Rev. Lett.* **89**, 246802 (2002).
43. Grigorenko, A. N., Roberts, N. W., Dickinson, M. R. & Zhang, Y. Nanometric optical tweezers based on nanostructured substrates. *Nature Photon.* **2**, 365–370 (2008).
44. Righini, M. *et al.* Nano-optical trapping of Rayleigh particles and *Escherichia coli* bacteria with resonant optical antennas. *Nano Lett.* **9**, 3387–3391 (2009).
45. Visscher, K., Gross, S. P. & Block, S. M. Construction of multiple-beam optical traps with nanometer-resolution position sensing. *IEEE J. Sel. Top. Quant. Electron.* **2**, 1066–1076 (1996).
46. Ashkin, A., Dziedzic, J. M. & Yamane, T. Optical trapping and manipulation of single cells using infrared laser beams. *Nature* **330**, 769–771 (1987).

47. Creely, C., Volpe, G., Singh, G., Soler, M. & Petrov, P. Raman imaging of floating cells. *Opt. Express* **13**, 6105–6110 (2005).

48. Rao, S., Bálint, S., Cossins, B., Guallar, V. & Petrov, D. Raman study of mechanically induced oxygenation state transition of red blood cells using optical tweezers. *Biophys. J.* **96**, 209–216 (2009).

49. Li, T., Kheifets, S., Medellin, D. & Raizen, M. G. Measurement of the instantaneous velocity of a Brownian particle. *Science* **324**, 1673–1675 (2010).

50. Ashkin, A. & Dziedzic, J. M. Feedback stabilization of optically levitated particles. *Appl. Phys. Lett.* **30**, 202–204 (1977).

51. Simmons, R. M., Finer, J. T., Chu, S. & Spudich, J. A. Quantitative measurements of force and displacement using an optical trap. *Biophys. J.* **70**, 1813–1822 (1996).

52. Wallin, A. E., Ojala, H., Hæggström, E. & Tuma, R. Stiffer optical tweezers through real-time feedback control. *Appl. Phys. Lett.* **92**, 224104 (2008).

53. Homola, J., Yee, S. S. & Gauglitz, G. Surface plasmon resonance sensors: Review. *Sensor. Actuator. B* **54**, 3–15 (1999).

54. Raschke, G. *et al.* Biomolecular recognition based on single gold nanoparticle light scattering. *Nano. Lett.* **3**, 935–938 (2003).

55. Larsson, E. M., Alegret, J., Kall, M. & Sutherland, D. S. Sensing characteristics of NIR localized surface plasmon resonances in gold nanorings for application as ultrasensitive biosensors. *Nano Lett.* **7**, 1256–1263 (2007).

56. Jonsson, M. P., Jonsson, P., Dahlin, A. B. & Hook, F. Supported lipid bilayer formation and lipid-membrane-mediated biorecognition reactions studied with a new nanoplasmonic sensor template. *Nano Lett.* **7**, 3462–3468 (2007).

57. Chen, S., Svedendahl, M., Käll, M., Gunnarsson, L. & Dmitriev, A. Ultrahigh sensitivity made simple: nanoplasmonic label-free biosensing with an extremely low limit-of-detection for bacterial and cancer diagnostics. *Nanotechnology* **20**, 434015 (2009).

58. Yang, A. H. J. *et al.* Optical manipulation of nanoparticles and biomolecules in sub-wavelength slot waveguides. *Nature* **457**, 71–75 (2009).

59. Sainidou, R. & García de Abajo, F. J. Optically tunable surfaces with trapped particles in microcavities. *Phys. Rev. Lett.* **101**, 136802 (2008).

60. Zhang, W., Huang, L., Santschi, C. & Martin, O. J. F. Trapping and sensing 10 nm metal nanoparticles using plasmonic dipole antennas. *Nano Lett.* **10**, 1006–1011 (2010).

61. Juan, M. L., Gordon, R., Pang, Y., Eftekhar, F. & Quidant, R. Self-induced back-action optical trapping of dielectric nanoparticles. *Nature Phys.* **5**, 915–919 (2009).

62. Genet, C. & Ebbesen, T. W. Light in tiny holes. *Nature* **445**, 39–46 (2007).

63. García-Vidal, F. J., Moreno, E., Porto, J. A. & Martín-Moreno, L. Transmission of light through a single rectangular hole. *Phys. Rev. Lett.* **95**, 103901 (2005).

64. García-Vidal, F. J., Martín-Moreno, L., Moreno, E., Kumar, L. K. S. & Gordon, R. Transmission of light through a single rectangular hole in real metal. *Phys. Rev. B* **74**, 153411 (2006).

65. García de Abajo, F. Light transmission through a single cylindrical hole in a metallic film. *Opt. Express* **10**, 1475–1484 (2002).

66. Kwak, E. S. *et al.* Optical trapping with integrated near-field apertures. *J. Phys. Chem. B* **108**, 13607–13612 (2004).

67. Baev, A. *et al.* Laser nanotrapping and manipulation of nanoscale objects using subwavelength apertured plasmonic media. *J. Appl. Phys.* **103**, 084316 (2008).

68. Blanco, L. A. & Nieto-Vesperinas, M. Optical forces near subwavelength apertures in metal discs. *J. Opt. A* **9**, 235–8 (2007).

69. Enoch, S., Quidant, R. & Badenes, G. Optical sensing based on plasmon coupling in nanoparticle arrays. *Opt. Express* **12**, 3422–3427 (2004).

70. Jain, P. K. & El-Sayed, M. A. Noble metal nanoparticle pairs: effect of medium for enhanced nanosensing. *Nano Lett.* **8**, 4347–4352 (2008).

71. Verellen, N. *et al.* Symmetry breaking in a plasmonic metamaterial at optical wavelength. *Nano Lett.* **9**, 1663–1667 (2009).

72. Liu, N. *et al.* Planar metamaterial analogue of electromagnetically induced transparency for plasmonic sensing. *Nano Lett.* **10**, 1103–1107 (2010).

73. Evlyukhin, A. B. *et al.* Detuned electrical dipoles for plasmonic sensing. *Nano Lett.* **10**, 4571–4577 (2010).

74. Balykin, V. I., Letokhov, V. S. & Klimov, V. V. Atom nano-optics. *Opt. Photon. News* **16**, 44–48 (2005).

75. Klimov, V. V., Sekatskii, S. K. & Dietler, G. Laser nanotraps and nanotweezers for cold atoms: 3D gradient dipole force trap in the vicinity of scanning near-field optical microscope tip. *Opt. Commun.* **259**, 883–887 (2006).

76. Chang, D. E. *et al.* Trapping and manipulation of isolated atoms using nanoscale plasmonic structures. *Phys. Rev. Lett.* **103**, 123004 (2009).

### Acknowledgements

This work was partially supported by the Spanish Ministry of Sciences under grants FIS2010-14834 and CSD2007-046-NanoLight.es, the European Community's Seventh Framework Programme under grant FP7-ICT-248835 (SPEDOC) and Fundació privada CELLEX.